Molecular Crystals and Liquid Crystals

Publication details, including instructions for authors and subscription information:
http://www.tandfonline.com/loi/gmcl20

Polymeric Composites Based on Polysilanes for Plastic Electronics

S. Nešpůrek [a], J. Pospíšil [a], I. Kratochvílová [b] & J. Sworakowski [c]

[a] Institute of Macromolecular Chemistry AS CR, Czech Republic

[b] Institute of Physics AS CR, Czech Republic

[c] Institute of Physical and Theoretical Chemistry, Wroclaw University of Technology, Wroclaw, Poland

Version of record first published: 22 Sep 2010

To cite this article: S. Nešpůrek, J. Pospíšil, I. Kratochvílová & J. Sworakowski (2008): Polymeric Composites Based on Polysilanes for Plastic Electronics, Molecular Crystals and Liquid Crystals, 484:1, 265/[631]-290/[656]

To link to this article: http://dx.doi.org/10.1080/15421400801904682

Mol. Cryst. Liq. Cryst., Vol. 484, pp. 265/[631]–290/[656], 2008

ISSN: 1542-1406 print/1563-5287 online
DOI: 10.1080/15421400801904682

Polymeric Composites Based on Polysilanes for Plastic Electronics

S. Nešpůrek[1], J. Pospíšil[1], I. Kratochvílová[2], and J. Sworakowski[3]
[1]Institute of Macromolecular Chemistry AS CR, Czech Republic
[2]Institute of Physics AS CR, Czech Republic
[3]Institute of Physical and Theoretical Chemistry, Wroclaw University of Technology, Wroclaw, Poland

The article reviews photophysical and photochemical properties of polysilanes – silicon backbone σ-conjugated polymers. Polysilanes have been of considerable research interest because of their electrical, optical and photoelectrical properties. Some of them seem to be prospective for the construction of electronic devices, like electroluminescent diodes, photodetectors, templates for oriented films of liquid crystals, molecular switches and phototransistors. Because of the effect of π-electron delocalization along the chain, they are good charge transporting materials and therefore good models for molecular wires. Their physical properties and chemical stability can be modified by side groups and by additives of different chemical structures.

Keywords: charge transport; composites; electronic structure; photoconductivity; plastic electronics; polysilane

INTRODUCTION

Polysilanes (sometimes called polysilylenes, polyorganosilanes, poly(silanediyl)s, organo-polysilanes, or catena-silicon polymers) have

This work was supported by the Grant Agency of the Academy of Sciences of the Czech Republic (grant No. IAA100100622) and by the Ministry of Education, Youth and Sports of the Czech Republic (grants No. 1041/2006-32 and No. CZ-24 – Czech-Polish collaboration), and by the Ministry of Science and Higher Education of Poland (grant No. 3 T08E 084 30). The authors thank the scientists participating in BIMORE (Bio-inspired Molecular Optoelectronics) project for valuable discussions and Ms. D. Dundrova for technical assistance.

Address correspondence to S. Nešpůrek, Institute of Macromolecular Chemistry AS CR, v. v. i., Heyrovsky Sq. 2, 162 06 Prague 6, Czech Republic. E-mail: nespurek@imc.cas.cz

been of considerable research interest because of their electronic properties and the effect of σ-electron delocalization along the chain [1]. Their electrical and optical properties differ significantly from structurally analogous carbon-based σ-bound systems, like polystyrene and polyethylene, rather resembling fully π-conjugated systems, like polyacetylenes. The charge delocalization is responsible for the effective charge carrier transport; on-chain charge carrier mobility reaches the value $\sim 10^6\,m^2\,V^{-1}\,s^{-1}$, 3D value was found to be of the order of $10^{-8}\,m^2\,V^{-1}\,s^{-1}$. Generally, polysilanes are not very stable under UV irradiation. However, the stability can be improved by various types of photostabilizing additives. On the other hand the photodegradation can be utilized for photoresist applications or in the process of surface photoorientation.

In this article we summarize the results of our recent activities in the field of electroactive polysilanes. Physical properties of polysilanes can be modified by side groups and by additives of various chemical structures. Some examples are discussed in the paper. Several polysilanes seem to be prospective for the construction of electronic devices, like electroluminescent diodes, photodetectors, molecular switches, phototransistors and templates for the oriented films of liquid crystals. Additives often play an important role.

MATERIALS AND CHEMICAL SYNTHESIS

Currently, the efficient synthesis of high molecular weight polysilanes is the Wurtz coupling of dichlorosilanes [2] (Scheme 1(a)). The molar mass of the polymer can be modified by the reaction temperature. However, this reaction has several drawbacks. First, the Wurtz coupling gives low yields (5–60%) and variable molecular weights. Secondly, the harsh conditions of the synthesis make the incorporation of the monomer functionalized by polar side groups on the monomer difficult or even impossible. Thus only a limited number of functionalized monomers can be used.

An alternative and less hazardous method was described by Aitken *et al.* [3]. Titanium and zirconium metallocene complexes were found to perform dehydrogenative coupling on phenylsilane to form oligo(phenylsilylene). Its Si–H bonds undergo mild free-radical hydrosilations across a wide variety of primary olefins and carbonyl compounds [4] according to Scheme 1, reaction (b). This synthesis paves the way to syntheses of novel polysilanes inaccessible by the Wurtz coupling method. Copolymers can be prepared in a similar way. Di-organodichlorosilanes are treated with metallic sodium, in a hydrocarbon diluent [5] at temperatures above 100°C, according to

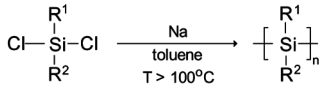

(a)

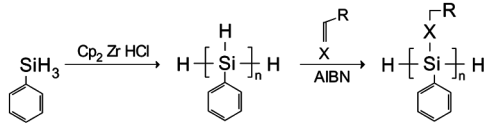

(b)

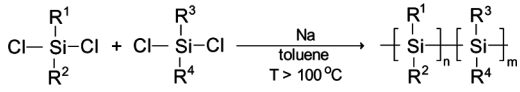

(c)

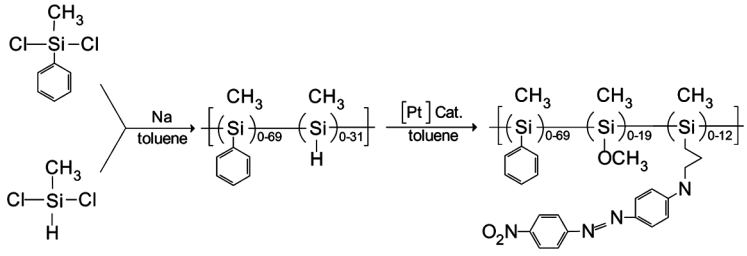

(d)

SCHEME 1 Chemical synthetic routes of the preparation of polysilanes and their copolymers.

Scheme 1, reaction (c). Because the groups R^1–R^4 can include a wide variety of aryl and alkyl groups, the number of possible kinds of polysilane copolymers is very large.

Recently, Tang and Qin [6] reported fully functionalized polysilane copolymers for photorefractive applications prepared by the Wurtz coupling and subsequent hydrosilylation (see Scheme 1, reaction (d)). We attempted to prepare new polysilane copolymers by chloromethylation and formylation of poly[methyl(phenyl)silylene] (PMPSi) (see Scheme 2, structure (3)) and subsequent condensation reactions of the aldehydic derivative (6) [7]. The formulae of the new derivatives of PMPSi we have obtained and used for discussions in this article are shown in Scheme 2 (structures (6)–(11); since several materials

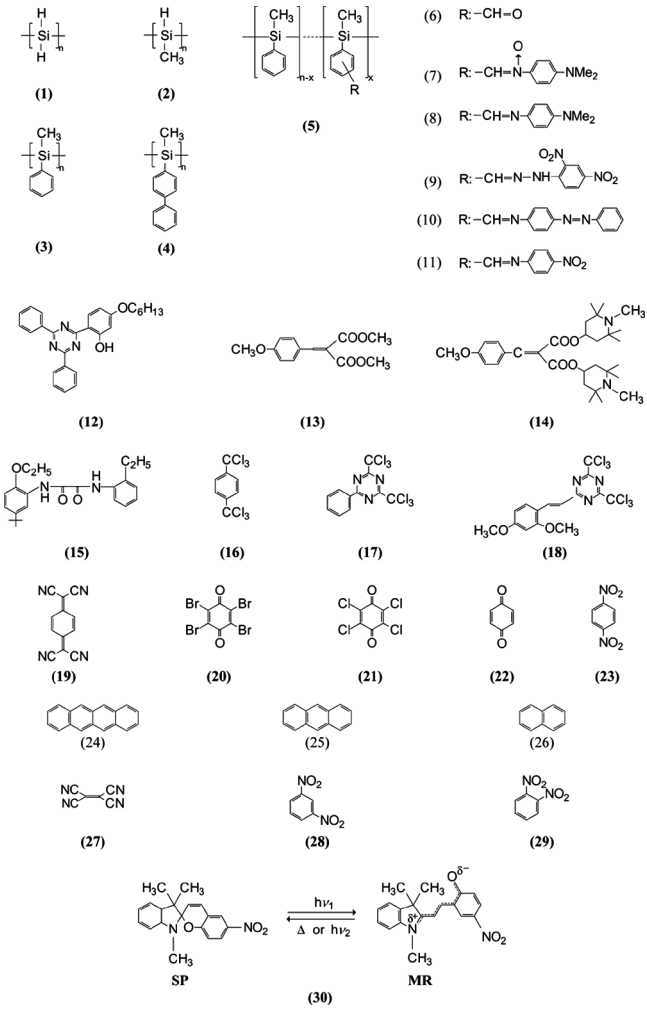

SCHEME 2 Chemical structures of materials discussed in this article.

will be mentioned in this paper, their chemical structures are presented in Scheme 2). Chloromethylation of PMPSi [1] using $CH_3OCH_2Cl/SnCl_4$ proceeded smoothly, but with some degradation of the main chain (usually to M_w between 20 000 and 30 000 g mol^{-1}).

Attempts to convert (5) (R: CH_2Cl) into (6) directly, using either oxidation with dimethyl sulfoxide or the Sommelet reaction resulted only in ill-defined oligomeric or crosslinked products. Therefore, we exploited the Kroehnke procedure, used in the past for the syntheses

of chemically sensitive aldehydes [8]. Polymer (5) (R: CH_2Cl) was first converted to quaternary salt (5) (R: CH_2–pyridinium chloride) using pyridine. This intermediate reacted with 4-nitroso-*N*,*N*′-dimethylaniline yielding nitrone (7) which smoothly hydrolyzed in acidic media to the aldehyde (6). This method was found to be feasible for (5) (R: CH_2Cl) with a degree of chloromethylation up to 0.25. Molar mass, M_w, of the polymeric aldehyde (6) was between 15 000 and 30 000. Condensation reactions of (6) with amines leading to Schiff bases (10), (11), as well as conversion (6) to (8) and preparation of 2,4-dinitrophenylhydrazone (9) proceeded smoothly and practically without degradation of the main chain. High degree of conversion was checked by IR, UV and visible spectra and by elemental analysis. On the other hand, the Witting reaction of (6) did not proceed satisfactorily and about half of the originally present aldehydic groups were still present even after long reaction times.

SAMPLE PREPARATION AND MEASUREMENTS

Procedures concerning the sample preparations for various types of studies and measurement details were described in our former papers [9–13]; thus we will not describe them here in detail. Electrical conductivity was measured using Keithley 6617A electrometer/high resistance meter. Transient photocurrent and charge carrier mobility measurements were performed by the time-of-flight (TOF) technique [9,10]. The quantum generation efficiency was determined by the xerographic discharge method [11]. UV-VIS-NIR absorption [12] was measured with a Perkin Elmer/Hitachi 340 spectrometer, infrared spectra [13] were measured with an FTIR spectrometer Bruker IFS 55.

ELECTRONIC STRUCTURE

The simplest polysilane is shown in Scheme 2, structure (1). However, this material is not stable and some substitution is necessary, for example with methyl groups (structure (2) in Scheme 2). Absorption UV spectrum consists of one peak, with maximum at about 310 nm. It has been shown that this absorption band reflects mainly delocalized (σ-σ^*) transitions of the Si backbone [1]. The energy of these transitions is conformation-dependent and is strongly influenced by the effective conjugation length of the macromolecule. The substitution with π-conjugated groups (e.g., phenyls) changes markedly the absorption spectrum (see Fig. 1a for poly[methyl(phenyl)silylene] (PMPSi) (structure (3) in Scheme 2). The absorption resulting from (σ-σ^*) transitions is shifted to long wavelength region, $\lambda_{max} = 338$ nm for solid

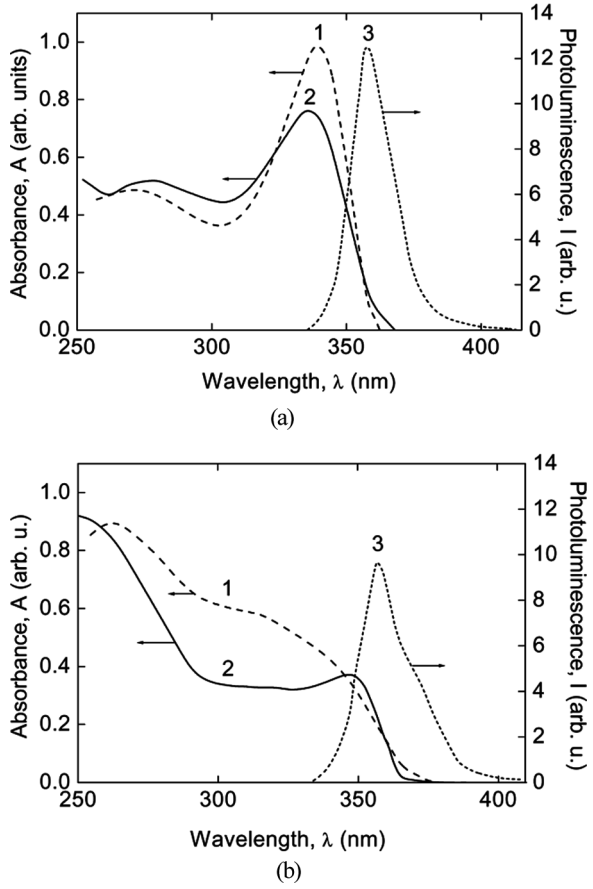

FIGURE 1 Absorption and fluorescence spectra of PMPSi (a) and PBMSi (b); curve 1 – in tetrahydrofuran solution, curve 2 – in the solid state, curve 3 – fluorescence spectrum in tetrahydrofuran solution.

PMPSi films [14,15]; the contribution of (π-π^*) transitions is weak. In polymers with fused-ring aryl substituents (e.g., naphthyl, biphenylyl), this absorption is better characterized as a localized (π-π^*) excitation with participation of a weaker (σ-σ^*) one (see Fig. 1b for (poly[biphenyl(methyl)silylene] (PBMSi) (structure (4) in Scheme 2). The (π-π^*) aryl-like excitations are responsible for the shorter wavelength absorption (maximum at $\sim$276 nm for solid PMPSi). Using an $(h\nu \times \alpha)^2$ vs. $h\nu$ plot (α is the absorption coefficient, h is the Planck constant and ν is the frequency of light), the optical band gap has been estimated as $E_g = 3.5$ eV. From fluorescence emission measurements,

the photoluminescence of PMPSi consists of a relatively sharp band with a maximum at 357 nm (see Fig. 1a) and of a broad emission in the visible region [16]. The latter is enhanced at low temperatures and during excitation with short wavelength light ($(\pi\text{-}\pi^*)$ absorption). At least four sub-bands were detected at low temperatures in PMPSi films. They are related to: (i) charge transfer $^1(\sigma,\pi^*)^{CT}$ states (410–500 nm); (ii) branching points, (iii) electron hole tail state transitions, and (iv) defect metastable states formed by backbone deformation or bond scission ($\lambda = 520 - 540$ nm). The detailed picture of the electron transitions was described elsewhere [17]. It follows from the excitation spectrum that direct radiationless deactivation processes from both the $^1(\pi,\pi^*)$ and $^1(\sigma,\pi^*)^{CT}$ states can occur. Chemically attached side groups can change energies of excited states, in consequence changing the shape of the absorption and photoluminescence spectra, ionization potential and electron affinity (and hence positions of HOMO and LUMO levels), energy of charge-transfer states and positions of energy levels of positive and negative polarons. The situation is shown in Figure 2. Curve 1 represents the absorption spectrum of PMPSi. Absorption spectrum of the functionalized polymer (9) (see Scheme 2), poly[methyl(phenyl)silylene/{3(4)-[(2,4-dinitrophenylhydrazono)methyl] phenyl}methylsilylene (PMPSi-DNPH) is shown as curve 2. Curve 3 is characteristic of the absorption spectrum of the chromophoric substituent. The shift of the maximum of the curve 2 with respect the position of the maximum of curve 3 into the long wavelength

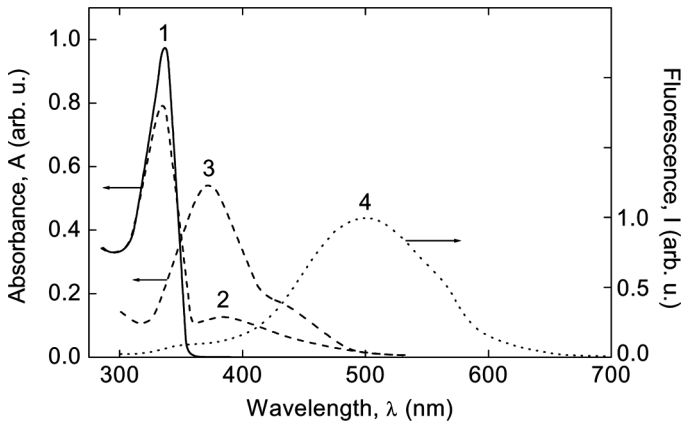

FIGURE 2 Optical absorption spectra of PMPSi (curve 1) and copolymer (9) (see Scheme 2, substitution degree 10^{-6} mol%, curve 2) in toluene solutions. Curve 3 – spectrum of the chromophore (concentration 1×10^{-6} mol l^{-1}), curve 4 – fluorescence of the copolymer (9).

region suggests the electronic interactions of the main chain and side groups. A similar shift of the maximum was observed in photoluminescence spectrum (cf. curve 4 in Fig. 2 and curve 3 in Fig. 1a). Concerning additives, one can change the energy position of charge-transfer states and therefore the efficiency of electron transfer, energy distribution of transport hopping states and positions of electron and hole localized states (traps). However, the exploitation of the effects strongly depends on the positions of HOMO and LUMO levels of the polymer and the additive.

INFLUENCE OF SIDE GROUPS AND ADDITIVES ON SOME PROPERTIES OF POLYSILANES

Chemical structure of side groups chemically attached to the Si backbone and the presence of additives strongly influence the photochemical stability and electronic properties of polysilanes. We will demonstrate some examples.

Photochemical Stability

Polysilanes are generally considered as photochemically unstable materials. Note, however, that these materials are quite stable in the dark and even under a weak light exposure, the Si–Si bond scission occurring under a strong UV irradiation. This property can be utilized in photolitography. Note that in litography, in addition to degradation process, the crosslinking plays an important role. At present, the conventional photo-, electron- or γ-radiation litography has feature tires about 100 nm. Structures of less than 10 nm may be fabricated by using techniques of shadowing and edge-step deposition [18]. In this way polysilanes seem to be prospective litographic materials. The photochemical routes which lead to the chain degradation are shown in Scheme 3 for PMPSi. The irradiation of PMPSi film in the region of the first absorption band (step (I) in Scheme 3) results in the formation of in-chain radicals and/or delocalized cation radicals (steps (II) and (III) in Scheme 3) [19,20] with strong transient absorption at around 460 and 370 nm. The kinetics of the radical decays suggests that they can recombine, but products based on photoinduced Si–Si bond scission can also occur. An irradiation in air can cause the formation of siloxane species ((IV) in Scheme 3) as follows from IR spectrum where additional peaks at 1122 and 1111 cm^{-1} were found and attributed to isolated and cumulated siloxane moieties, respectively [13]. The passage (II) $\rightarrow$ (IV) is a complex process including several interstages as follows from IR studies [12]. Here, carbonyl

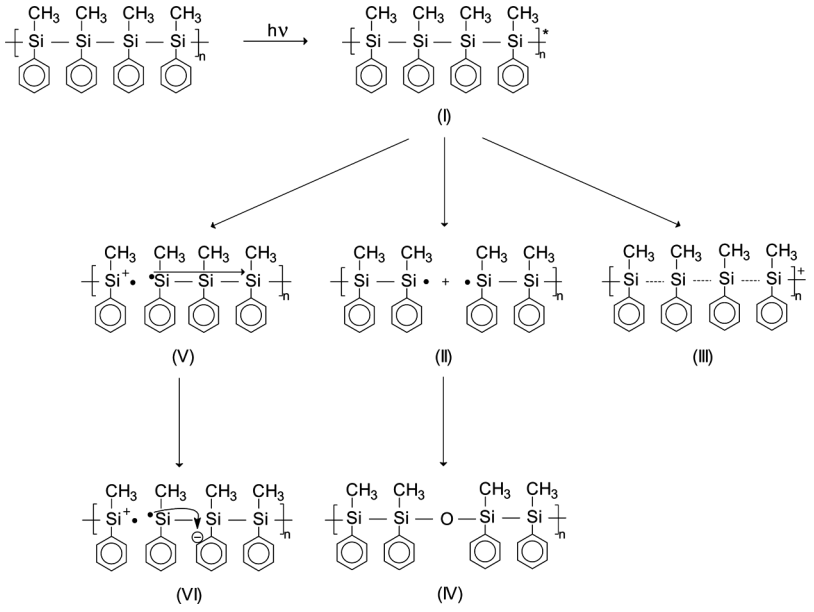

SCHEME 3 Formation of photospecies during the (σ-σ^*) excitation of PMPSi.

and hydroxyl species were detected. The proposed mechanism is shown in Scheme 4. Silyls II are able to recombine in oxygen-free atmosphere. In the presence of air, a sequence of photooxidation processes proceeds via peroxyl III, hydroperoxide IV, its photolysis to silyloxyl radical IX and recombination of the latter with II to siloxane moiety XI, forming the principal photooxidation-borne species. The silyloxyl radical IX serves also as a source of silanol X. Formation of the carbonyl species VIII, another minority product, is suggested to be formed via benzyl radical V, its autooxidation to peroxyl VI and photolysis of hydroperoxide VII. Formation of a carbosilane link $Si-CH_2-Si$ via interaction between carbon-centered radical V and silyl II, creating a component of a crosslink XII cannot be excluded. We paid attention to development of siloxane function and the related effects of photostabilizers.

During (σ-σ^*) excitations, i.e. the excitations of Si–Si bonding electrons, the electron can be promoted from the bonding to an antibonding orbital. This process can be followed by an electron transfer on the polymer chain ((V), Scheme 3). Thus, an electron-hole pair is formed. However, the pairs generated in the same chain segment very often recombine geminately with a very fast decay rate ($k_1 \approx 1.2 \times 10^7\ s^{-1}$)

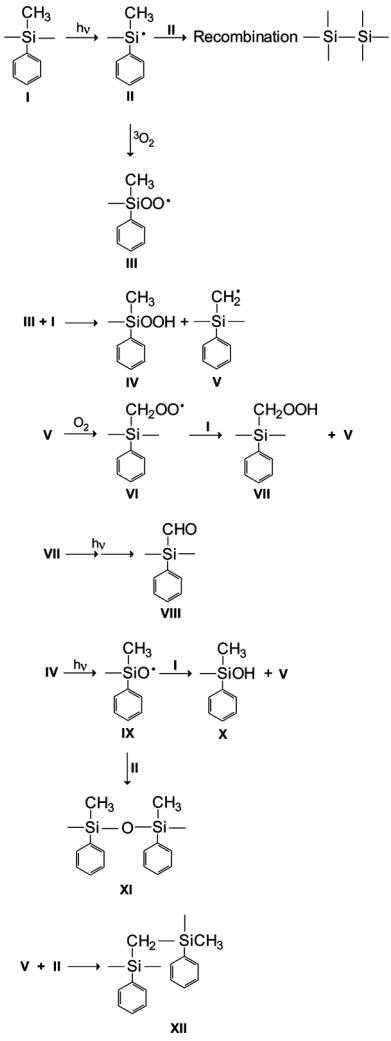

SCHEME 4 Chemical reactions during the development of PMPSi photodegradation and formation of polysiloxane structure.

due to the charge delocalization in the backbone. An intrachain ((VI), Scheme 3) or interchain electron transfer is necessary for the stabilization of the charge transfer state. The electron transfer from the polysilane chain to aryl is quite probable as follows from the data of photoelectron spectroscopy and electrochemistry [21–24]. A similar situation exists during the (π-π^*) excitation of phenyl groups, where a Frenkel exciton is

formed. A positive hole from the excited phenyl group is transferred to the Si–Si backbone and a main chain cation-radical is formed.

The photodegradation of polysilanes associated with changes in the absorption spectrum were detected (Fig. 3a). The intensity of the long wavelength band, which arises from the delocalized (σ-σ^*) electronic transitions, decreases with the progress of the photodegradation and has its maximum shifted to shorter wavelengths [25]. Because the energy of this transition is conformation-dependent and depends on the molar mass and conjugation length of the macromolecule, the excitation energy is effectively deposited almost exclusively in the longest all-trans segments. Thus, the blue shift of the peak suggests that Si–Si bond scission occurred and conjugation length became shorter. This was demonstrated by measurements of the decrease in molar mass during the PMPSi and PBMSi (poly[biphenyl(methyl) silylene]) photodegradation [9] (see Fig. 4) and by photoluminescence experiments [16]. The exposure with the linearly polarized light results in the angularly dependent excitation of the main chain segments, oriented parallel to the electric field vector of the exciting light. Figure 3b shows the polar diagram of the absorbance at 333 nm after irradiation with linearly polarized light of 335 nm. An anisotropic distribution of long time species is clearly visible. This process can be utilized for liquid crystal alignment.

Evidently, the larger π-conjugated side groups stabilize the polymer [7]. The situation was also observed with functionalized polymers (6), (9)–(11) (see Scheme 2). The results are summarized in Table 1.

There are two important effects concerning the chain stabilization: (i) Higher polaron binding energy [26,27] leading to an enhanced stability, (ii) The improved stability requiring a conjugation between the main chain and side groups for reversible (resonant) electron transfer from the side group to the main chain. In addition to the stabilization of polysilanes with π-conjugated side groups it is possible to achieve a better stability by admixing suitably chosen additives. The resistance against photooxidation can be increased by UV absorbers; see structures in Scheme 2: (12), 2-(4,6-diphenyl-1,3,5-triazin-2-yl)-5-(hexyloxy)phenol (Tinuvin 1577), (13), dimethyl[(4-methoxyphenyl)methylidene]propanedioate (Hostavin PR 25), and (15) *N*-(4-*tert*-butyl-2-ethoxyphenyl)-*N*′-(2-ethylphenyl)oxalanilide (Sanduvor EPU). The strong triazine-based phenolic UV absorber (12) and oxalanilide-based stabilizer (15) protect the polymer also by excited state intramolecular proton transfer (ESIPT) mechanism. The UV absorber (13) provides only a negligible protection. The degradation changes could be rather effectively retarded by the addition of bifunctional stabilizer (14), bis(1,2,2,6,6-pentamethyl-4-piperidinyl)-2-[(4-methoxyphenyl(methylene]malonate, which combines

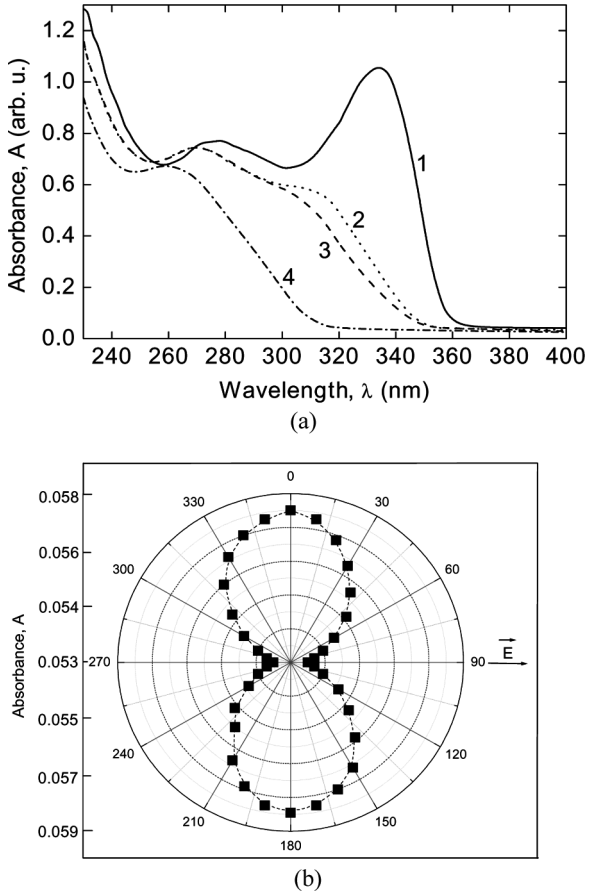

FIGURE 3 (a) Changes in polarized UV spectra of PMPSi film on irradiation with linearly polarized light of He-Cd laser ($\lambda = 325$ nm, $P = 10$ mW cm^{-2}): (1) spectrum of as-prepared film; (2) spectrum parallel to the polarization of the exciting light after the exposure dose 0.2 J cm^{-2}; (3) spectrum perpendicular to the polarization of the exciting light after the exposure dose 0.2 J cm^{-2}; (4) spectrum measured after the exposure dose 12.0 J cm^{-2}. (b) Polar diagram of the absorbance at 333 nm after the irradiation with linearly polarized light of 333 nm (HBO 100 W, 7 min). Vector $\vec{E}$ visualizes the electric field vector of the incident light.

the function of UV absorber with HAS (hindered amine stabilizer, radical scavenger). IR analysis indicates that the phototriggered irreversible degradation of PMPSi consists mainly of dual photoprocesses – photolysis and photooxidation – followed by the conversion of the primary

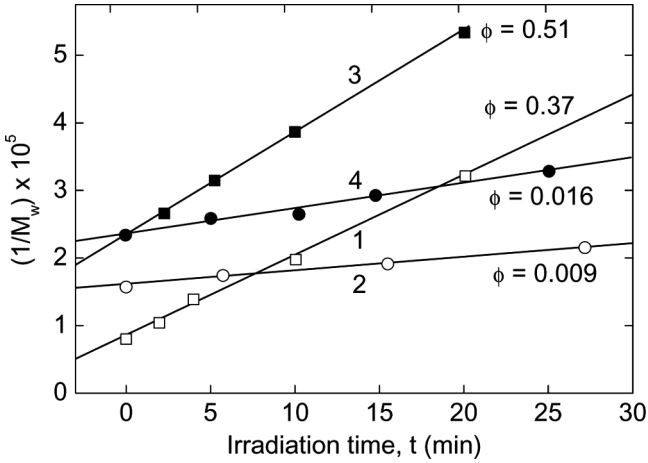

FIGURE 4 Reciprocal value of the molar mass (determined by gel permeation chromatography) of PMPSi and PBMSi vs. irradiation time; $\lambda_{inc} = 350$ nm. Line 1 – solid PMPSi, line 2 – solid PBMSi, line 3 – PMPSi tetrahydrofuran solution, line 4 – PBMSi tetrahydrofuran solution. ϕ stands for the quantum efficiency of polymer main chain scission.

species. Main attention was paid to changes in siloxane formation which can be effectively reduced by application of the phenolic UV (12) and oxanilide (15) absorbers and/or their combination with HAS in cooperative systems [28].

For some applications (e.g., photolitography) a fast degradation is necessary. It can be reached by special additives (see structures (16), (17) and (18) in Scheme 2). All these materials are rich in chlorine.

TABLE 1 Photodegradation of Poly[methyl(phenyl)silylene] Functionalized Polymers as Measured by the Relative Absorbance A/A_0 (%) at λ_{max} after UV Irradiation ($\lambda = 330$ nm, photon flux $= 9.8 \times 10^{17}$ photon $m^{-2} s^{-1}$)

Polymer (see Scheme 2)	THF solution[a]	Solid film[b]
(3)	12	56
(8)	25	69
(9)	89	90
(10)	97	95
(11)	96	96

[a] 5 min irradiation.
[b] 40 min irradiation.

A comparison of the structures (12) and (17) suggests that an irreversible electron transfer from PMPSi chain to the additive could play an important role. The probability of this process strongly depends on the relative positions of LUMO levels. This finding needs more investigations.

Charge Carrier Transport

The important parameter of the electrical conductivity is charge carrier mobility, the basic parameter of the charge carrier transport. Charge carrier transport in polysilanes can be described by the model of disordered polarons, i.e., by hopping of positive charged species [26,27,29–31]. We will describe first the charge transport in unsubstituted PMPSi.

Linear Si backbone behaves as a molecular wire due to the σ-conjugation. The macroscopic zero-field mobility in PMPSi is of the order of $10^{-8}\,m^2\,V^{-1}\,s^{-1}$ but the microscopic ("on-chain") mobilities are much higher. The highest "on-chain" mobilities were detected as $2\times10^{-5}\,m^2\,V^{-1}\,s^{-1}$ [32]. The velocities of mobile charges (holes) depend on the chemical nature and on the size of the side groups. In alkyl-substituted polysilanes, the hole mobilities seem to increase with the increasing length of the alkyl substituent; for example, in poly[hexyl(phenyl)silylene] (PHPSi), the "on-chain" mobility equal to $2\times10^{-5}\,m^2\,V^{-1}\,s^{-1}$ was reported, whereas $\mu < 10^{-6}\,m^2\,V^{-1}\,s^{-1}$ was found for poly[ethyl(phenyl)silylene] (PEPSi) by the time-resolved microwave conductivity technique [32]. The film crystallinity plays an important role in this case. The "on-chain" hole mobility in poly[methyl(phenyl)silylene] was found to amount to ca. $2\times10^{-6}\,m^2\,V^{-1}\,s^{-1}$ using time-resolved microwave photoconductivity [29].

A question arises why the values of "on-chain" mobilities, albeit quite high as compared with other polymers, are so much lower from the respective values of crystalline silicon. A possible reason is the formation of polarons. The strong electron-phonon coupling causes carrier self-trapping and creates a quasiparticle, a polaron, which can move only by carrying along the associated molecular deformation. The motion of such a charge carrier, dressed into a cloud of local deformation of the nuclear subsystem, can be phenomenologically described by introducing a temperature-dependent effective mass which is higher than the electron mass. A significant distortion of the PMPSi chain was found by Kim *et al.* [33] by measuring the migration rate of the excitation energy along the polymer chain. The dependence of the charge carrier drift mobility, μ, on the electric field strength, F, in a 3D PMPSi sandwich sample could be described by an exp $(\beta F^{1/2})$

dependence for $F > 10^7\,\mathrm{V\,m^{-1}}$. At lower field strengths, $\mu(F)$ becomes constant or increases slightly upon reducing F [10,30]. These types of dependences are usually treated in the framework of the hopping disorder concept. The essential difference between the polaron and disorder models is that the latter one, at variance with the former one, implies a sufficiently weak electron-phonon coupling and the activation energy of charge transport reflects the static energy disorder of the hopping sites. In contrast, the polaron model suggests a strong electron-phonon coupling and a negligible contribution of energy disorder to the activation energy of the carrier mobility. Since the structural distortion is an intramolecular process, the polaron binding energy E_p is not subjected to any meaningful variation. Concomitantly, the polaronic charge transport must obey the Gaussian statistics and the photocurrent transients should neither feature a long tail nor become dispersive at any temperature. It was suggested [9,26,30] that the zero-field mobility, $\mu(T, F \to 0)$, can be approximated by the sum of the polaron and disorder contribution as

$$\mu(T, F \to 0) = \mu_0 \exp\left[-\left(\frac{E_p}{2kT} + \frac{4}{9}\frac{\sigma^2}{(kT)^2}\right)\right] \tag{1}$$

where σ is the energy width of the distribution of transport hopping states, k is the Boltzmann constant, T is the temperature and μ_0 is the mobility pre-factor. Usually it is difficult to distinguish from experimental data between $\mu(1/T)$ and $\mu(1/T^2)$ dependences. Then, the exponential term in Eq. (1) is usually treated as a temperature-dependent contribution to the apparent (effective) activation energy $E_a^{eff} = E_p/2 + (8/9)\,\sigma^2/kT$.

It follows from Eq. (1) that the activation energy of the mobility will be higher (and, therefore, charge mobility lower) if the polaron binding energy will be higher and distribution of density of hopping states broader. The former parameter depends on molecular charge-phonon interactions and deformation of the molecule during charging. Thus, to keep high charge mobility the molecule must contain small number of chemical bonds, i.e., must be small and rigid (polymer chain must not be flexible). High free volume of the material and large freedom of side groups are responsible for a large deformation of the molecule, high polaron binding energy and, therefore, for a low charge mobility.

As follows from Figure 5, the charge carrier mobility can be modified by additives (see Fig. 5, chemical structures of the additives see Scheme 2). The value of the mobility depends on the electron affinity (see Fig. 5b) and additive concentration c. The square-root field dependence is still conserved. Note that for naphthalene (26) and

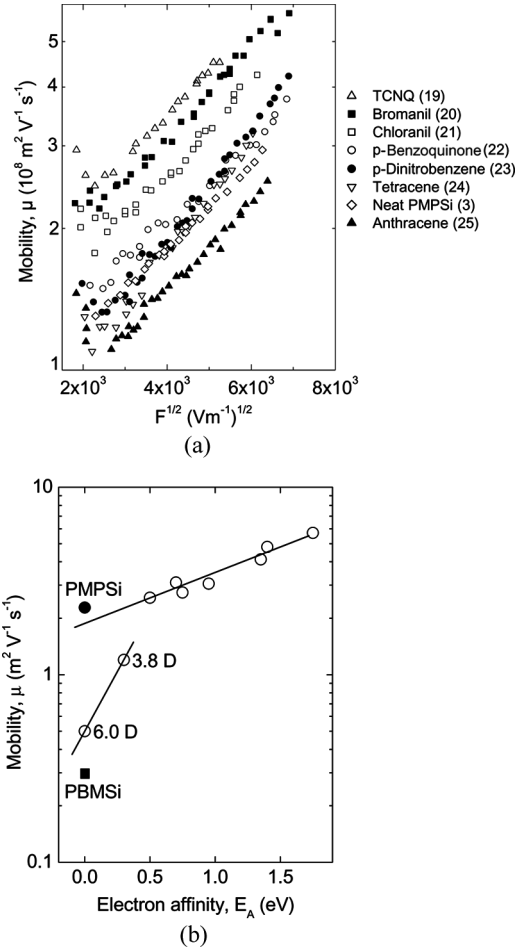

FIGURE 5 (a) The charge carrier mobility vs. the square root of the electric field strength for neat PMPSi (◇) and PMPSi with various additives (3 mol%); (b) The charge carrier mobility of doped PMPSi films vs. the electron affinity of the dopants. Full circle – charge mobility μ of undoped PMPSi, full square – charge mobility μ of undoped PBMSi. Electric field strength $3.6 \times 10^7\,\mathrm{V\,m^{-1}}$. The chemical structures of additives – see numbering in Scheme 2.

tetracyanoethylene (27) the mobility values decreased on the values $5 \times 10^{-9}\,\mathrm{m^2\ V^{-1}\ s^{-1}}$ and $3 \times 10^{-9}\,\mathrm{m^2\,V^{-1}\,s^{-1}}$, respectively, at the field $F = 1.6 \times 10^7\,\mathrm{V\,m^{-1}}$.

Two materials with electron affinity 0.3 and 0.0 eV (m-dinitrobenzene (28) and o-dinitrobenzene) (29)) exhibit an unusual behaviour

(see Fig. 5b). They are materials with quite high dipole moment, 3.8 and 6.0 D, respectively. This effect needs some explanation and will be discussed in more detail. Two effects are important in the presence of dipolar species in the material: (i) Broadening of the distribution of the density of hopping states; (ii) Dispersion of polarization energy of the solid in the presence of dipolar species.

In the case of the broadening of the distribution of the density of hopping states the statistical transport level for charge carriers moves to the Fermi level and mobility decreases [34]. Mathematically, this fact can be written in the form (see Eq. (2))

$$\mu = \mu_0 \exp\left[-\left(\frac{2\sigma_{real}}{3kT}\right)^2\right] \tag{2}$$

μ_0 being usually identified with the mobility in a parent perfect material (on-chain mobility in the case of polymers). The effect of dipolar species has been rationalized invoking a dipolar contribution σ_{dip} as

$$\sigma_{real}^2 = \sigma^2 + \sigma_{dip}^2 \tag{3}$$

where the latter component is related to the permanent dipole moment of the polar species and its mole fraction x [35–37].

$$\sigma_{dip} = \frac{\kappa x^b m}{\varepsilon a_0^2}. \tag{4}$$

Here, κ and b are constants, ε is the relative electric permittivity of the medium, and a_0 is the inter-site distance. Taking the parameters of Hirao and Nishizawa [37] ($\kappa = 8.35$; $b = 2/3$) with $\varepsilon = 3$, and assuming other relations as above, one arrives at the ratio of the mobilities in the material without and with dipoles $\mu/\mu^{(dip)} \approx 2.2$ at ambient temperature.

The value of the polarization energy [38] consists of several terms, namely from the interactions of ion (localized charge) – induced dipole, localized charge-permanent dipole, permanent dipole – induced dipoles, etc. These result in both the broadening of the distribution of transport electronic states and the formation of new localized states with energy E_t for charge carriers (dipolar traps). They influence the charge mobility according to the formula

$$\mu = \mu_0 \left[1 + \exp\left(\frac{E_t}{kT}\right)\right]^{-1} \tag{5}$$

It follows from calculations performed on a model crystal lattice [39] that the trap depth is a linear function of the dipole moment, being

0.5 eV for additives with the dipole moment 10 D. Assuming $x \approx 0.01$ (corresponding to the inter-dipole distance equal to ca. 5 lattice constants of a typical molecular crystal (e.g., anthracene) and taking the depths of traps 0.5 eV, one arrives the decrease of the mobility six orders of magnitudes at ambient temperature.

When dipolar species are formed by light, e.g., using a photochromic additive, an optoelectric switch can be constructed [40]. We have performed two experiments using spiropyrane (SP) molecule (3′,3′-dimethyl-6-nitro-2,3-dihydrospiro(benzothiazole-2,2′-[2H]chromene)), which changes after UV exposure to zwitterionic highly polar merocyanine MR, (3-methyl-2-(1-methyl-2(5-nitro-2-oxidophenyl)vinyl-benzothiazol-3-ium)) (see reaction (30) in Scheme 2). According to quantum chemical calculations [41], during this photochemical conversion the dipole moment changes from 5 to 11 D. Simultaneously a new band arises in absorption spectrum with maximum at 590 nm. This change results in a reversible decrease of electrical current by ca. 1 order of magnitude.

An opposite trend of changes can be observed upon doping PMPSi with acceptor species. Because PMPSi is a hole semiconductor, additives of acceptor type can increase the conductivity. As an example for the "doping," we present the experiment with exposure to iodine. After 40 min treatment of PMPSi film with iodine vapors, the conductivity increased up to $10^{-4}\,\mathrm{S\,cm^{-1}}$.

Charge Carrier Photogeneration – Photoconductivity

An increase of electrical conductivity upon sample illumination (photoconductivity) usually arises from a change in the density of free carriers (Δn). If the incident light creates g carriers per second per unit volume of a photoconductor, then the steady-state value of Δn equals $g\tau$, where τ is the lifetime of a charge carrier, g can be written as a product $g = \eta\alpha\Phi$, where η is the quantum photogeneration efficiency, α is the absorption coefficient and Φ is the total absorbed radiation (photons per square metre per second). Under the assumption that charge carrier mobility, μ, is unaffected by the excitation, the photocurrent in a solid provided with ohmic contacts is given by the formula:

$$i_{ph} = \sigma_{ph}\boldsymbol{F} = e\eta\alpha\Phi\mu\tau\boldsymbol{F} \tag{6}$$

where $\boldsymbol{F}$ is the electric field strength. Thus the photocurrent is a function of two main terms: the quantum efficiency η and the range of the charge carriers $\mu\tau\boldsymbol{F}$.

The process of charge carrier photogeneration is quite complex and very often includes several mechanisms. Here, we will discuss only

two basic mechanisms, viz., (i) charge generation due to HOMO-LUMO transitions and (ii) that via the autoionization process. We will not discuss the processes like exciton dissociation at the electrode/semiconductor interface, exciton dissociation due to the interaction of excitons with trapped charge carriers, exciton dissociation due to the interaction of excitons and impurities, and direct excitation of trapped carriers into the conduction or valence bands. The first step of charge carrier photogeneration is the photon absorption. It can be realized in the mechanism (i) on the main polymer chain or on side groups. Optical absorption in the main polymer chain is associated with HOMO-LUMO excitations – here, there is some similarity to band-to-band transitions in inorganic semiconductors. The excitation of the main chain results in formation of "on-chain" electron-hole pairs (see Scheme 3) that usually undergo a fast geminate recombination to a significant extent. The remaining portion of the pairs escape the fast geminate recombination presumably due to the fact that the chain conjugation extents only over a limited number of chemical bonds. The remainder of electron-hole pairs relaxes to the ion-pair charge-transfer states (CT). This implies a transfer of the electron from the backbone to the pendant side group (intramolecular CT state) or to another polymer chain (intermolecular CT state). The formation of intermolecular CT state is based on electron transfer to another macromolecule or some impurity molecule (e.g., oxygen). From the point of view of energy structure, the CT states are polar states localized below conduction band (LUMO level, electron) and above valence band (HOMO level, hole). Electron and hole in the CT state are bound by Coulomb interaction and can move by stochastic hopping through polymer bulk.

Under the influence of the external electric field, ion pairs can dissociate creating free charge carriers. This step involves the thermal dissociation of the electron-hole (ion) pair into free carriers by Brownian motion subject to the connected action of the Coulomb and applied fields. The fraction of absorbed photons resulting in bound thermalized pairs is the primary quantum yield η_0 which is supposed to be independent of the electric field. Under this assumption the overall field dependence of the photogeneration is governed by the efficiency of the dissociation step which may be described using the solution of the Smoluchowski equation given by Onsager [42,43]. According to this model, the dependence of the quantum efficiency on applied field is strongly superlinear. The experimental results are shown in Figure 6. The full lines represent the best theoretical fits to our experimental data for PMPSi (curve 2) and PBMSi (curve 1) for 355 nm irradiation. Fitting parameters were: for PMPSi: separation

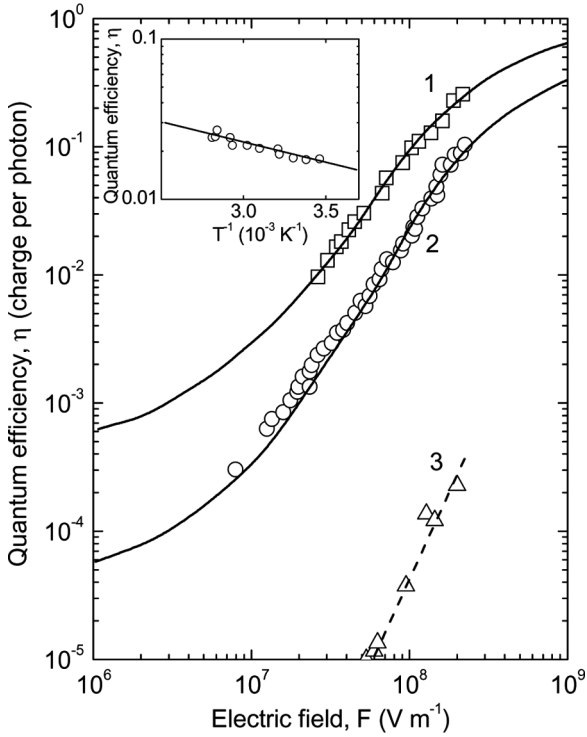

FIGURE 6 The electric field dependence of the photogeneration efficiency ($T = 300$ K) in PMPSi (curve 2) and PBMSi (curve 1) under 355 nm illumination. The full lines were calculated using the Onsager dissociation theory [42]. For comparison, several points taken for poly(dihexylsilylene) are presented (curve 3). Inset: The temperature dependence of the quantum efficiency for PMPSi.

distance of positive and negative charge [43] $\beta = 1.3$ nm, primary quantum efficiency, i.e., fraction of ion-pairs generated by one photon $\eta_0 = 0.45$; for PBMSi $\beta = 1.6$ nm, $\eta_0 = 0.85$. This result demonstrates that the larger π-conjugated side groups, the higher is the quantum efficiency. The temperature dependence of η (see inset in Fig. 6) is also in a good agreement with the Onsager theory. The results indicate that the Onsager model of the geminate recombination is a good description of the field and temperature dependences of the photogeneration efficiency. The presence of an acceptor facilitates the photoinduced electron transfer. Very often oxygen molecules or photooxidation products present in the bulk of the polymer sample participate in the photogeneration mechanism.

The measurements of charge photogeneration in PMPSi with various chemically attached side groups (see copolymers (7)–(9) and (11) in Scheme 2) measured by the electrographic technique of emission-limited photoinduced discharge [11] give the following values of the generation efficiences (room temperature, $F = 2 \times 10^7\,\mathrm{V\,m^{-1}}$, $\lambda = 355\,\mathrm{nm}$) [44]: neat PMPSi, $\eta = 8 \times 10^{-3}$ charge per photon; (9), $\eta = 3 \times 10^{-2;}$ (11), $\eta = 5 \times 10^{-2;}$ (7) and (8), $\eta = 1.2 \times 10^{-3}$. An increase of the photogeneration efficiency was observed for polysilanes with acceptor-like side groups (copolymers (9) and (11)). For copolymers (7) and (8) containing dimethylaminophenyls, i.e., donor groups, η was found to be about one order of magnitude lower than that for neat PMPSi. Similarly, as in the case of neat PMPSi, the electric field dependence of η could be described by usual Onsager model. As compared with PMPSi, large effective separation distances were obtained for polysilane functionalized polymers (9) and (11) and lower ones for (7) and (8). The electron acceptor groups in the side polymer chains effectively increase the ion-pair separation distances, limit the geminate recombination and increase the quantum efficiency η.

A similar effect of acceptors and donors was observed with additives [45]. The quantum efficiencies η were roughly proportional to half-wave reduction potentials, I_R, of the additives. The fraction of charge carrier on one absorbed photon was found to be following (the applied electric field was $2 \times 10^7\,\mathrm{V\,m^{-1}}$). Net PMPSi without additive ($\eta = 7 \times 10^{-4}$ charge/photon), PMPSi + 9,10-phenanthrenequinone ($\eta = 10^{-3}$ charge/photon $I_R = -0.66\,\mathrm{V}$), PMPSi + 1-(benzylideneamino)-4-nitronaphthalene ($\eta = 10^{-3}$ charge/photon), PMPSi + 1,4-dicyanobenzene ($\eta = 5 \times 10^{-3}$ charge/photon), PMPSi + 2,3-dichloro-5,6-dicyanobenzene ($\eta = 6 \times 10^{-3}$ charge/photon, $I_R = -0.01\,\mathrm{V}$), PMPSi + tetrachloro-1,4-benzoquinone ($\eta = 8 \times 10^{-3}$ charge/photon $I_R = -0.51\,\mathrm{V}$). The set of experimental dependencies of η on electric field strength is shown for other additives in Figure 7. Note that the increase of the charge efficiency was observed even for tetracene (24), which supports the idea of the unusual behaviour of the silicon backbone.

Possible Model Devices

Polysilanes have generally been considered as photochemically unstable materials. The findings of some types of side groups and additives which stabilize the Si chain opens the field for possible applications. Because of quite complicated syntheses, the use of additives represents a simpler way of changing chemical and physical behaviour of polysilanes. Using photoabsorbers and radical scavengers (see structures (12)–(15) in Scheme 2) allows one to prepare stable polymer

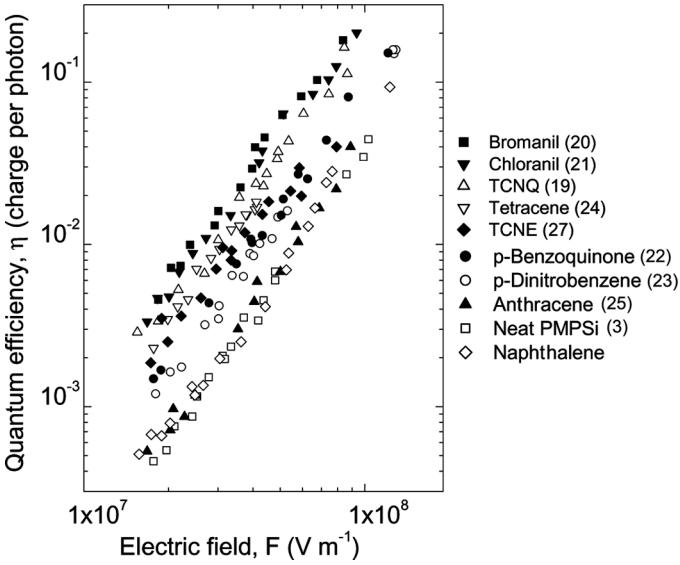

FIGURE 7 Quantum efficiency of charge carrier generation η vs. electric field strength for neat PMPSi and PMPSi doped with 3 mol% additive, excitation wavelength $\lambda = 339$ nm. The chemical structures of additives – see numbering in Scheme 2. The measurements were performed by time-of-flight method. Note that η values are a little lower than those obtained by the emission-limited photoinduced discharge method.

films (note that the concentration of the additives is not too high and physical properties of the polymer are mostly preserved). On the other side, the litographic applications need fast photo-, electron-, and γ-degradation; this process can also be optimized by using appropriate additives.

The degradation process can also be utilized in the process of surface orientation of thin films, consisting of both the photodegradation of Si chains, formation of long lived dipolar species of cation radicals of the main chain and anion radicals of side groups [25] and formation of metastable electronic states [17]. Polysilane (especially PMPSi) surface treated in this way can be used for the photoalignment of liquid crystals [46] and the preparation of polarized electroluminescence diodes [47]. The spectral change in photoluminescence during the formation of metastable states can be used for the fabrication of optical switches [48]. Because of quite high carrier mobility, polysilanes can be used as charge transporting materials; the possible use is in copy machines and light emitting diodes (even in UV region). The limitation

of charge carrier mobility in the presence of dipolar additives allows us to construct photoelectrical switch if photochromic additive is used [49]. Surface photopotential generated by photochemical transformation of photochromic species can substitute gate electrode in FET devices [50]. Quite high quantum generation efficiency, and hence high photoconductivity, allows us to construct photodetectors. Another potential use is seen in the field of non-linear optics, holography and photorefractivity.

Photorefractive (PR) media are multifunctional materials which combine photoconductivity and electro-optical activity to manifest the photorefractive effect [51]. Generally, there are four basic processes involved in the photorefractive effect: the charge photogeneration, the transport of the generated charge carriers by thermal diffusion and/or by field-assisted drift, the trapping of the charge carriers which results in the formation of the space charge field, and the formation of a phase grating due to space charge field modulation of the refractive index via the linear electro-optical effect. It should be noted that two light beams are needed to generate the spatially modulated space charge field. It is believed that PR polymers will possess unique properties, like easy preparation of the samples, low electric permittivity, high optical performance and low cost. Two approaches have been developed to fabricate PR media: the multi-component material approach and the fully functionalized polymer. The multi-component systems can be easily prepared from different materials but their use may pose several problems, such as their intrinsic instability due to phase separation. Although fully functionalized polymer systems also exhibit several disadvantages, they offer advantages like a stable transparency, minimum phase separation and high stability of the dipole orientation. The rationale for designing PR materials with conjugated backbones is that the backbone plays the triple role of charge generator, charge transporter and backbone senso stricto. Thus, the four functions necessary to exhibit the photorefractive effect exist simultaneously in a single polymer. Furthermore, the use of conjugated backbones enhances the density of NLO chromophores. As an example we can mention the copolymer (10) (see Scheme 2).

In the following we will present two examples illustrating attempts to optimize the photorefractive parameters. Because of the solubility of additives it is suitable to use poly(diorganylsilylene)s with large, relatively polar side groups, e.g., butoxyphenyl group instead of non-substituted phenyl ring. This substitution very often leads to an improved optical quality of thick polymer films, too. Experimental results of Silence *et al.* [52] show that poly[(4-butoxyphenyl)

ethylsilylene] as the host charge-transporting polymer with the non-linear chromophore Coumarin-153 or *N*-diethyl-2-fluoro-4-((E)-2-nitroprop-1-en-1-yl)aniline and the sensitizing agent C^{60} or trinitrofluorenone gives a steady-state diffraction efficiency of 10^{-4} at $\lambda = 753\,\text{nm}$, under the electric field $F = 16\,\text{V mm}^{-1}$ in a 175 mm thick sample. The characteristic response time of the initial rise was 39 ms at $\lambda = 647\,\text{nm}$ (writing intensity of $1\,\text{W cm}^{-2}$, $F = 11.4\,\text{V mm}^{-1}$). The response was limited by the charge generation and not by the mobility. Hendrickx *et al.* [53] prepared various polysilane copolymers functionalized with the optically nonlinear chromophore N-methyl-p-nitroaniline. Asymmetric two-beam coupling was observed at 622 nm, and a gain coefficient of $18\,\text{cm}^{-1}$ was measured at an externally applied field of $4.8 \times 10^4\,\text{V m}^{-1}$. These examples suggest that one can forecast use of polysilanes as future optoelectronic materials.

CONCLUSION

Polysilanes are generally considered as photochemically unstable materials. However, these polymers are quite stable in the dark and even under weak light exposure. We have found a way of limiting the level of photodegradation using some special types of side groups and additives, like UV absorbers, and bifunctional stabilizers combining the functions of UV absorbers and radical scavengers. Polysilanes are excellent charge transporting materials with relatively high mobilities, negligible trapping, and high photoconductivity and photoluminescence in the UV region. Metastable states, similar to those encountered in amorphous silicon, can be generated by illumination; this allows the construction of luminescence switching devices. It is an advantage that physical properties of polysilanes can be modified not only by side groups chemically attached to the silicon backbone but also by additives. This feature facilitates tailoring of the properties to the needs of possible devices.

REFERENCES

[1] Miller, R. D. & Michl, J. (1989). *Chem. Rev.*, *89*, 1359.
[2] Zhang, X. H. & West, R. (1984). *J. Polym. Chem. Ed.*, *22*, 159.
[3] Aitken, C. I., Harrod, J. F., & Samuel, E. (1986). *J. Am. Chem. Soc.*, *108*, 4059.
[4] Hsiao, Y. L. & Waymouth, R. M. (1994). *J. Am. Chem. Soc.*, *116*, 9779.
[5] West, R. (1986). *J. Organomet. Chem.*, *300*, 327.
[6] Tang, H. D. & Qin, J. G. (2000). *Chinese Chem. Lett.*, *11*, 675.
[7] Kmínek, I., Nešpůrek, S., Brynda, E., Pfleger, J., Cimrová, V., & Schnabel, W. (1993). *Collect. Czech. Chem. Commun.*, *58*, 2337.

[8] Kroehnke, F. (1953). *Angew. Chem.*, *65*, 612.
[9] Nešpůrek, S. & Eckhardt, A. (2001). *Polym. Adv. Technol.*, *12*, 427.
[10] Nešpůrek, S., Valerián, H., Eckhardt, A., Herden, V., & Schnabel, W. (2001). *Polym. Adv. Technol.*, *12*, 306.
[11] Nešpůrek, S. & Ulbert, K. (1975). *Czech. J. Phys.*, *25A*, 144.
[12] Meszároš, O., Schmidt, P., Pospíšil, J., & Nešpůrek, S. (2006). *Polym. Degrad. Stabil.*, *91*, 573.
[13] Meszároš, O., Schmidt, P., Pospíšil, J., & Nešpůrek, S. (2004). *J. Polym. Sci. Ser. A, Polym. Chem.*, *42*, 714.
[14] Harrah, L. A. & Zeigler, J. M. (1987). *Macromolecules*, *20*, 610.
[15] Navrátil, K., Šik, J., Humlíček, J., & Nešpůrek, S. (1999). *Opt. Mater.*, *12*, 105.
[16] Nešpůrek, S., Schauer, F., & Kadashchuk, A. (2001). *Chem. Monthly*, *132*, 159.
[17] Nešpůrek, S., Wang, G., Schauer, F., & Kajzar, F. (2006). *Mol. Cryst. Liq. Cryst.*, *447*, 265.
[18] Brodie, I. & Muray, J. J. (1992). *The Physics of Micro/Nano-Fabrication*, Plenum Press: New York.
[19] Nešpůrek, S., Herden, V., Schnabel, W., & Eckhardt, A. (1998). *Czech. J. Phys.*, *48*, 477.
[20] Irie, S. & Irie, M. (1992). *Macromolecules*, *25*, 1766.
[21] Pitt, C. G., Carey, R. N., & Toren Jn., E. C. (1972). *J. Am. Chem. Soc.*, *94*, 3806.
[22] Turner, D. W., Baker, C., Baker, A. D., & Brundle, C. R. (1970). *Molecular Photoelectron Spectroscopy*, Wiley-Interscience: London.
[23] Bock, H. & Ensslin, W. (1971). *Angew. Chem. Int. Ed.*, *10*, 404.
[24] West, R. (1971). *Organosilicon Symposium*, Pittsburgh.
[25] Nešpůrek, S., Zakrevskyy, Y., Stumpe, J., Sapich, B., & Kadashchuk, A. (2006). *Macromolecules*, *39*, 690.
[26] Fischuk, I. I., Kadashchuk, A., Bassler, H., & Nešpůrek, S. (2003). *Phys. Rev.*, *B67*, 224303.
[27] Arkhipov, V. I., Emelianova, E. V., Kadashchuk, A., Blonsky, I., Nešpůrek, S., Weiss, D. S., & Bässler, H. (2002). *Phys. Rev.*, *B65*, 165218.
[28] Meszároš, O., Schmidt, P., Pospíšil, J., Nešpůrek, S., & Kelnar, I. (2004). *Macromol. Symp.*, *212*, 335.
[29] Nešpůrek, S., Herden, V., Kunst, M., & Schnabel, W. (2000). *Synth. Met.*, *109*, 309.
[30] Bässler, H., Borsenberger, P. M., & Perry, R. J. (1994). *J. Polym.Sci. B: Polym. Phys.*, *32*, 1677.
[31] Nešpůrek, S., Sworakowski, J., Kadashchuk, A., & Toman, P. (2003). *J. Organomet. Chem.*, *685*, 269.
[32] Grozena, F. C., Siebbeles, L. D. A., Warman, J. M., Seki, S., Tagawa, S., & Scherf, U. (2002). *Adv. Mater.*, *14*, 228.
[33] Kim, Y. R., Lee, M., Thorne, J. R. G., Hochstrasser, R. M., & Zeigler, J. M. (1988). *Chem. Phys. Lett.*, *145*, 75.
[34] Valerián, H., Brynda, E., & Nešpůrek, S. (1995). *J. Appl. Phys.*, *7*, 6071.
[35] Dickmann, A., Bässler, H., & Borsenberger, P. M. (1994). *J. Chem. Phys.*, *99*, 8136.
[36] Young, R. H. & Fitzgerald, J. J. (1995). *J. Chem. Phys.*, *102*, 9380.
[37] Hirao, A. & Nishizawa, H. (1997). *Phys. Rev. B*, *56*, R 2904.
[38] Nešpůrek, S. & Sworakowski, J. (2001). *Thin Solid Films*, *339*, 168.
[39] Sworakowski, J. (2000). *IEEE Trans. Diel. Electr. Insul.*, *7*, 531.
[40] Sworakowski, J., Nešpůrek, S., Toman, P., Wang, G., & Bartkowiak, W. (2004). *Synth. Met.*, *147*, 241.
[41] Toman, P., Bartkowiak, W., Nešpůrek, S., Sworakowski, J., & Zalesny, R. (2005). *Chem. Phys.*, *316*, 267.

[42] Onsager, L. (1938). *Phys. Rev.*, *54*, 554.
[43] Nešpůrek, S. & Cimrová, V. (1988). *Prog. Colloid Polym. Sci.*, *78*, 88.
[44] Cimrová, V., Kmínek, I., Nešpůrek, S., & Schnabel, W. (1994). *Synth. Met.*, *64*, 271.
[45] Brynda, E., Nešpůrek, S., & Schnabel, W. (1993). *Chem. Phys.*, *175*, 459.
[46] Dyadyusha, A., Nešpůrek, S., Reznikov, Yu., Kadashchuk, A., Stumpe, J., & Sapich, B. (2001). *Mol. Cryst. Liq. Cryst.*, *359*, 67.
[47] Nešpůrek, S., Wang, G., Rais, D., Rakušan, J., Karásková, M., Stumpe, J., & Zakrevskyy, Y. (2006). *Mol. Cryst. Liq. Cryst.*, *448*, 1.
[48] Nešpůrek, S., Kadashchuk, A., Skryshevski, Yu., Fujii, A., & Yoshino, K. (2002). *J. Luminescence*, *90*, 131.
[49] Nešpůrek, S., Toman, P., & Sworakowski, J. (2003). *Thin Solid Films*, *268*, 438–439.
[50] Nešpůrek, S., Wang, G., Toman, P., Sworakowski, J., Bartkowiak, W., Iwamoto, M., & Combellas, C. (2005). *Mol. Cryst. Liq. Cryst.*, *430*, 127.
[51] Günter, P. & Huignard, J. P. (Eds.) (1998). *Photorefractive Materials and their Applications*, Springer-Verlag: Berlin.
[52] Silence, S. M., Scott, J. C., Hache, F., Ginsburg, E. J., Jenkner, P. K., Miller, R., Tweig, R. J., & Moerner, W. E. (1993). *J. Opt. Soc. Am. B*, *10*, 2306.
[53] Hendrick, E., Van Sternwinckel, D., Persoons, A., & Watanabe, A. (1999). *Macromolecules*, *32*, 2232.